

Aircraft Trajectory Dataset Augmentation in Latent Space

Seokbin Yoon¹ Keumjin Lee¹

Abstract

Aircraft trajectory modeling plays a crucial role in Air Traffic Management (ATM) and is important for various downstream tasks, including conflict detection and landing time prediction. Dataset augmentation through the addition of synthetically generated trajectory data is necessary to develop a more robust aircraft trajectory model and ensure that the trajectory dataset is sufficient and balanced. In this work, we propose a novel framework called ATRADA for aircraft trajectory dataset augmentation. In the proposed framework, a Transformer encoder learns the underlying patterns in the original trajectory dataset and converts each data point into a context vector in the learned latent space. The converted dataset in the latent space is projected into reduced dimensions using principal component analysis (PCA), and a Gaussian mixture model (GMM) is applied to fit the probability distribution of the data points in the reduced-dimensional space. Finally, new samples are drawn from the fitted GMM, the dimension of the samples is reverted to the original dimension, and they are decoded with a Multi-Layer Perceptron (MLP). Several experiments demonstrate that the framework effectively generates new, high-quality synthetic aircraft trajectory data, which were compared to the results of several baselines.

1. Introduction

As the demand for air transportation continues to increase around the world, the concept of air traffic operations has shifted to Trajectory-Based Operation (TBO). TBO more accurately manages an aircraft's four-dimensional trajectory (4DT) in latitude, longitude, altitude, and time. Many studies have developed data-driven aircraft trajectory models for various downstream applications such as conflict detection and landing time prediction (Liu & Hwang, 2011; Hong &

Lee, 2015).

One study on trajectory modeling suggested using a GMM to learn statistical patterns of aircraft trajectories (Barratt et al., 2018), while another study used a Long Short-term Memory (LSTM) network to learn aircraft trajectory patterns in the presence of various procedural constraints in airspace (Shi et al., 2020). Other research combined a Convolutional Neural Network (CNN) with an LSTM network to better extract spatio-temporal features in trajectories (Ma & Tian, 2020). Recently, various efforts have been made to apply Transformer-based architectures for trajectory prediction (Guo et al., 2022; 2024; Tong et al., 2023).

Due to the complex interactions between aircraft, air traffic controllers (ATCo) often manually assign specific headings, altitudes, and speeds to aircraft to ensure safe and efficient operation. This process is known as radar vectoring and results in diverse patterns in aircraft trajectories, as shown in Figure 1. However, ATCo can have particular preferences regarding how to deviate aircraft from predefined flight paths, which can lead to imbalance among different trajectory patterns. Figure 2 shows a histogram of different trajectory patterns for arriving aircraft at Inchon International Airport, South Korea, which illustrates the possibility of imbalance in the trajectory dataset. Such imbalance could deteriorate the performance of learning-based trajectory models and make them overfit major trajectory patterns. Therefore, it is beneficial to expand the dataset with synthetically generated data through dataset augmentation (Yoon & Lee, 2023).

Although a sufficient and balanced dataset is crucial for training data-driven aircraft trajectory models, very limited attention has been given to trajectory dataset augmentation. In this work, we propose a novel framework for aircraft trajectory dataset augmentation. The proposed framework consists of three parts. First, the original trajectory dataset is transformed into a learned latent space using a sequence autoencoder trained to reconstruct the input trajectory in its output. Various architectures, including a Sequence to Sequence (Seq2Seq) LSTM network (Sutskever et al., 2014), can be used as an autoencoder. However, we choose a Transformer-based architecture due to its superior representation capability for long sequences (Vaswani et al., 2017). Second, once the original trajectory dataset is transformed into a set of context vectors in the latent space, the proba-

¹Department of Air Transport, Transportation and Logistics, Korea Aerospace University, Goyang, South Korea. Correspondence to: Keumjin Lee <keumjin.lee@kau.ac.kr>.

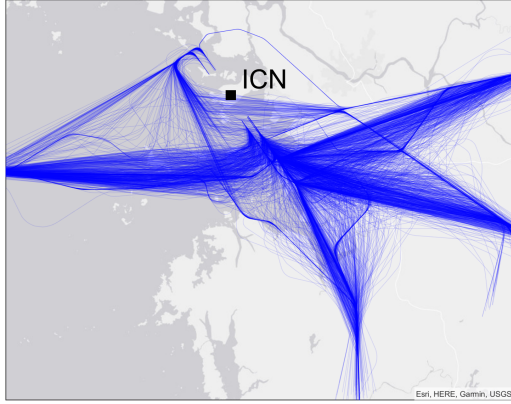


Figure 1. Actual aircraft trajectories at Incheon International Airport (ICN), South Korea, over a two-month period.

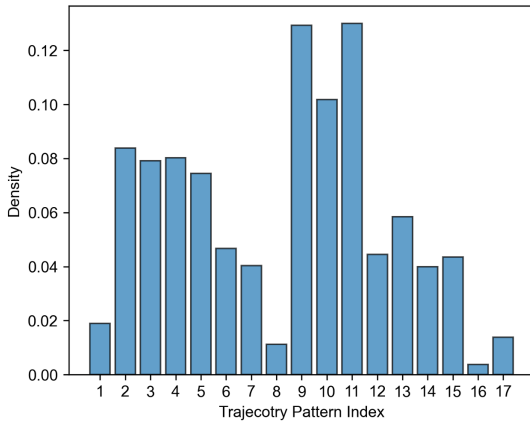


Figure 2. Densities of trajectories in Figure 1 for each trajectory pattern.

bility distribution of the vectors is fitted by a GMM. Lastly, new samples are drawn from the fitted GMM and decoded in the same manner as in the trajectory reconstruction process in the first step.

The main advantage of the proposed framework is that the underlying probability distribution of trajectory dataset in the latent space is explicitly estimated. By doing this, the newly augmented data can preserve the temporal dependency between trajectory points over time (i.e., aircraft dynamics) and the spatial flight patterns due to various operational constraints in specific airspace. The proposed framework for aircraft trajectory dataset augmentation is validated with actual air traffic surveillance data. Through a series of experiments, we demonstrate that the synthetic trajectory data generated by the proposed method outperform those by other generative models in both discriminative and predictive tasks.

2. Related Works

2.1. Time-series data generation

Several studies have applied Generative Adversarial Networks (GANs) (Goodfellow et al., 2014) to generate synthetic time-series data. One study used LSTM networks as both a generator and discriminator. A noise vector was used as input, and time-series data were generated recursively (Mogren, 2016). A similar approach was applied in another study, where more realistic time-series data were generated using a Recurrent Neural Network (RNN) with additional domain-specific inputs (Esteban et al., 2017). TimeGAN was proposed to better preserve the temporal dynamics in the time-series training data, and both reconstructive and adversarial objectives were jointly optimized (Yoon et al., 2019).

The Variational Autoencoders (VAEs) have been explored for time-series data generation. TimeVAE was introduced to enable user-defined distributions in the decoder and enrich the temporal properties of the generated data (Desai et al., 2021). The representation capabilities of transformers have led to their adoption in time-series generation tasks. For example, Museformer was designed with fine- and coarse-grained attention mechanisms for symbolic music generation (Yu et al., 2022). Another study combined an adversarial autoencoder with a Transformer to generate time-series data by integrating local and global features in the data (Srinivasan & Knottenbelt, 2022).

2.2. Aircraft trajectory generation

The generation of synthetic aircraft trajectories presents significant challenges because they need to capture both the temporal dynamics of aircraft movement and the spatial distribution while respecting various operational constraints within a specific airspace. For example, arriving aircraft should pass through specific three dimensional fixes and maintain appropriate altitudes to ensure safe and efficient landing. One such critical point is the Final Approach Fix (FAF), which marks the beginning of the final approach segment where pilots initiate their final descent for landing, as illustrated in Figure 3.

One study applied a GMM to fit the distribution of an aircraft trajectory dataset and generate synthetic trajectories by drawing samples from the fitted GMM (Barratt et al., 2018). Another study also applied a GMM and used a feature vector that consisted of deviations from a flight path rather than actual position measurements to better represent variability in trajectories within specific airspace (Jung & Kochenderfer, 2023). The synthetic minority over-sampling technique (SMOTE) (Chawla et al., 2002) was employed to augment aircraft trajectory data in minor trajectory patterns to improve the accuracy of trajectory prediction (Yoon &

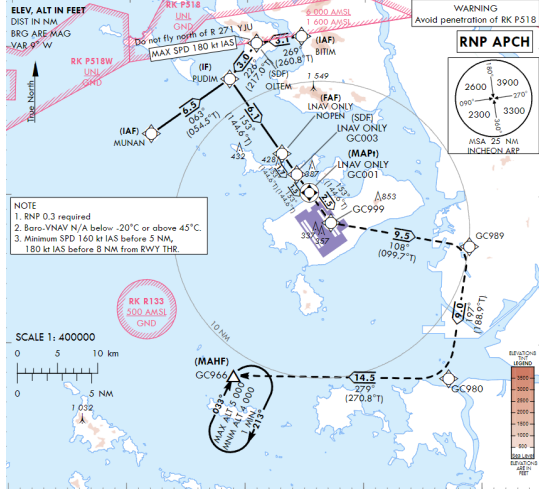


Figure 3. An example of operational constraints for arriving aircraft (Approach chart for ICN).

Lee, 2023). Another study combined a Temporal Convolutional Network (TCN) and a VAE for aircraft trajectory generation (Krauth et al., 2023).

3. Methodology

3.1. Background

3.1.1. SELF-ATTENTION MECHANISM

The self-attention mechanism is the heart of the Transformer (Vaswani et al., 2017) and mimics human cognitive processes by selectively focusing on specific elements within an input sequence. Attention mechanism is defined as:

$$\text{Attention}(\mathbf{Q}, \mathbf{K}, \mathbf{V}) = \text{softmax}\left(\frac{\mathbf{Q}\mathbf{K}^T}{\sqrt{d_k}}\right)\mathbf{V} \quad (1)$$

where \mathbf{Q} , \mathbf{K} , and \mathbf{V} represent queries, keys, and values, respectively, and d_k represents the dimension of the keys. The queries \mathbf{Q} interact with the keys \mathbf{K} through a dot-product operation and quantifies the relevance of each key to each query. This interaction produces attention weights that are normalized using the softmax function. These normalized weights are subsequently applied to the values \mathbf{V} , effectively contextualizing the input sequence. In practice, a multi-head attention is applied to provide a more diverse representation of the input sequence.

3.1.2. GAUSSIAN MIXTURE MODEL

The GMM is a probabilistic model that represents the probability distribution of a dataset as a mixture of multiple Gaussian distributions, each representing a distinct cluster.

of data points. The GMM is defined as:

$$p(\mathbf{t}) = \sum_{i=1}^K \pi_i \mathcal{N}(\mathbf{t}; \mu_i, \Sigma_i) \quad (2)$$

where t represents C -dimensional vector with a probability distribution comprising the weighted sum of K Gaussian distributions. Here, π_i denotes the mixture weight of the i^{th} Gaussian component with a constraint of the sum of all mixture weights being equal to 1. The parameters $\{\pi_i, \mu_i, \Sigma_i\}$ of each i^{th} Gaussian distribution are estimated using the Expectation-Maximization (EM) algorithm to maximize the likelihood of the observed data.

3.2. Proposed Framework

The proposed framework is illustrated in Figure 4. The framework consists of two main components: an autoencoder and a GMM. The autoencoder is trained to reconstruct the input trajectory and then used to convert the trajectory dataset from its original space into context vectors in the latent space. The decoder part of the autoencoder is used to synthesize new trajectory data from samples drawn from the GMM, which fits the probability distribution of the dataset in the latent space. Importantly, since the GMM training occurs after the autoencoder is fully trained, the generation results can be optimized without retraining the autoencoder by adjusting the associated hyperparameters (i.e., the number of principal components for PCA and the number of Gaussian distributions in the GMM).

3.2.1. SEQUENCE AUTOENCODER

For the sequence autoencoder, we utilize a Transformer-based encoder with a self-attention mechanism and a Multi-Layer Perceptron (MLP) as a decoder. As illustrated in Figure 4(a), we first embed the aircraft trajectory $\{\mathbf{x}_{1:S}^i\}_{i=1}^B \in \mathbb{R}^{B \times F \times S}$ into the embedding vectors with a hidden dimension D , where B is the mini-batch size, F is the number of original features (i.e., latitude, longitude, and altitude), and S is the maximum length of aircraft trajectory sequences. The embedded trajectory sequence $\{\mathbf{x}_e_{1:S}^i\}_{i=1}^B \in \mathbb{R}^{B \times D \times S}$ is then fed into the trajectory encoder.

The trajectory encoder employs the full self-attention mechanism, as proposed in the original Transformer model (Vaswani et al., 2017). This choice is based on long-term relationships between trajectory points at different timestamps being as crucial as their short-term relationships in air traffic operations. For example, the trajectory points in the early part of a sequence contain information about the entry point into the airspace and significantly influence the trajectory points at much later time steps due to the use of Standard Terminal Arrival Route (STAR). Finally, the latent vectors $\{\mathbf{z}_{1:S}^i\}_{i=1}^B \in \mathbb{R}^{B \times D \times S}$ from the trajectory encoder are passed into the decoder, where the aircraft tra-

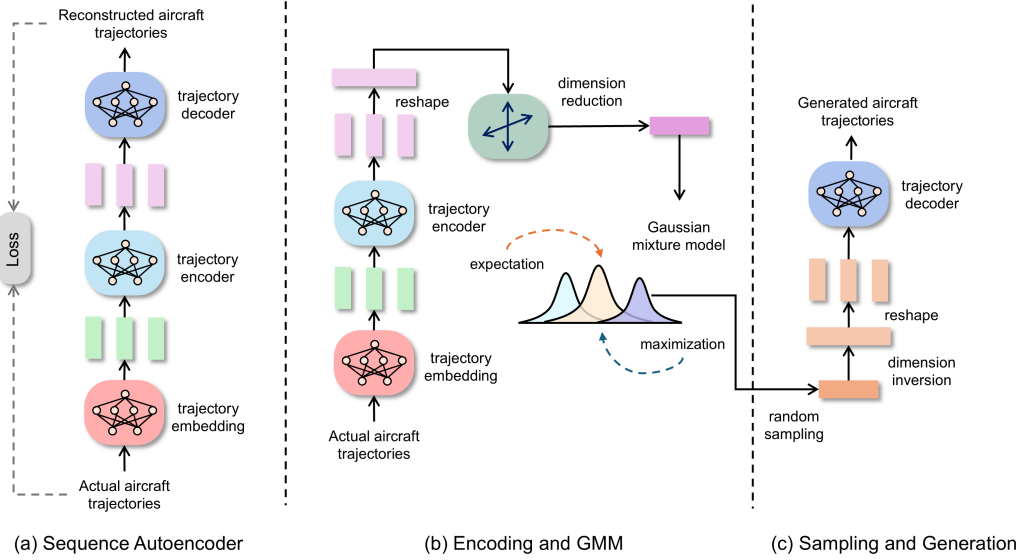


Figure 4. The proposed framework for aircraft trajectory dataset augmentation. (a) A sequence autoencoder learns latent space representations in an unsupervised way. (b) Aircraft trajectories are encoded, and GMM is fitted to the latent vectors. (c) Samples are randomly drawn from the fitted GMM and decoded for generation.

jectory is reconstructed as $\{\tilde{\mathbf{x}}_{1:S}^i\}_{i=1}^B \in \mathbb{R}^{B \times F \times S}$. We use L2 loss function, $\frac{1}{B} \sum_{i=1}^B \|\mathbf{x}^i - \tilde{\mathbf{x}}^i\|_2^2$, to measure the difference between the actual trajectories and the reconstructed trajectories. Notably, the use of the MLP in the trajectory decoder enables non-autoregressive trajectory generation. This significantly reduces the computation time and minimizes the risk of error accumulation, which typically occurs in other autoregressive times-series generative models.

3.2.2. ENCODING AND GMM

Once the autoencoder is fully trained, we encode the aircraft trajectory sequences $\{\mathbf{x}_{1:S}^j\}_{j=1}^N \in \mathbb{R}^{N \times F \times S}$ from the original dataset into latent vectors $\{\mathbf{z}_{1:S}^j\}_{j=1}^N \in \mathbb{R}^{N \times D \times S}$, where N is the total number of trajectories in the dataset. We then transpose the latent vector at each time step and concatenate them to form a row vector $\overrightarrow{\mathbf{z}}_j^j$ for each trajectory sequence:

$$\overrightarrow{\mathbf{z}}^j = \{\mathbf{z}_{j_1}^T \oplus \mathbf{z}_{j_2}^T \oplus \cdots \oplus \mathbf{z}_{j_S}^T\} \quad (3)$$

where $\overrightarrow{\mathbf{z}}^j \in \mathbb{R}^{1 \times (D \cdot S)}$, and \oplus denotes concatenation. We then stack $\overrightarrow{\mathbf{z}}^j$ row-wise, which results in a matrix $\mathbf{M} \in \mathbb{R}^{N \times (D \cdot S)}$. PCA is applied to this matrix, which results in a matrix $\mathbf{O} \in \mathbb{R}^{N \times P}$. Through PCA, the latent vectors $\overrightarrow{\mathbf{z}}^j$ are projected into a low-dimensional space ($1 \leq P < (D \cdot S)$), where the principal feature vectors are orthogonal to each other. This step helps to manage redundancy and noise in the dataset and facilitates the training of the GMM, which fits the matrix \mathbf{O} as a mixture of multiple Gaussian distributions $p(\mathbf{y}) = \sum_{i=1}^K \pi_i \mathcal{N}(\mathbf{y}; \mu_i, \Sigma_i)$.

3.2.3. SAMPLING AND GENERATION

To augment a dataset, new latent vectors $\{\mathbf{y}^q\}_{q=1}^M \in \mathbb{R}^{M \times P}$ are sampled from the fitted GMM, where M is the number of generated samples. They can then be reverted to the original dimension ($\mathbb{R}^{M \times P} \rightarrow \mathbb{R}^{M \times (D \cdot S)}$) and reshaped ($\mathbb{R}^{M \times (D \cdot S)} \rightarrow \mathbb{R}^{M \times D \times S}$) for decoding. Finally, new aircraft trajectory data $\{\tilde{\mathbf{y}}_{1:S}^q\}_{q=1}^M \in \mathbb{R}^{M \times F \times S}$ are generated as outputs of the decoder. Importantly, the new samples $\{\mathbf{y}^q\}_{q=1}^M$ can still be effectively decoded, as the multivariate Gaussian distribution $p(\mathbf{y})$ provides proper representations of the original dataset.

4. Numerical Experiments

The proposed framework was implemented in the following software and hardware environments: Python 3.9.16, PyTorch 2.0.1, CUDA 11.7, an Intel Core i7-12700F CPU, 32 GB of RAM, and an NVIDIA GeForce RTX 3060 GPU.

4.1. Dataset Description

We utilized trajectories of arriving aircraft in the terminal airspace (70-NM radius) at Incheon International Airport, South Korea. The dataset was acquired from FlightRadar24¹, which collects aircraft trajectory data via the Automatic Dependent Surveillance–Broadcast (ADS-B) system. The dataset covers the period from January 2022 to June 2022 and comprises a sequential record of the state of each aircraft. The data include details such as the time,

¹<https://www.flightradar24.com>

aircraft type, geographical position (latitude, longitude, and altitude), and other pertinent information. The ADS-B trajectory data have a non-uniform sampling rate, so we resampled the data using a piecewise cubic Hermite interpolating polynomial (PCHIP) (Fritsch & Carlson, 1980) so that it would have a uniform rate ($\Delta t = 6$ sec). Table 1 provides a description of the ADS-B trajectory dataset used in this work.

Table 1. ADS-B trajectory dataset description.

Attribute	Detail
Number of Seq	7,712
Dimension	3
Avg Seq Len	264 (1,584 sec)
Max Seq Len	271 (1,626 sec)
Features	Latitude, Longitude, Altitude

4.2. Model Configurations

We set the number of encoder layers to $L = 3$, the hidden dimension to $D = 128$, the number of heads to $h = 4$, the feedforward dimension to $D_{ff} = 512$, and the dropout probability to $p = 0.2$. For the training process, we used the ADAM optimizer (Kingma & Ba, 2017) with an initial learning rate of 10^{-4} . The number of principal components P for PCA was 22, which accounts for 99% of the variance in the dataset. The number of Gaussian distributions K of the GMM was determined as 32 based on the Bayesian Information Criterion (Schwarz, 1978).

4.3. Comparison Baselines

In this work, we compared the proposed framework with several competitive baselines: TimeGAN (Yoon et al., 2019), TimeVAE (Desai et al., 2021), SMOTE-Interpolation (SMOTE-I), SMOTE-Extrapolation (SMOTE-E) (DeVries & Taylor, 2017), GMM (Barratt et al., 2018) and TCN-VAE (Krauth et al., 2023). We utilized the following publicly available source code for the implementation of the baselines (TimeGAN, TimeVAE, TCN-VAE and GMM). Upon the publication of this paper, our source code for ATRADA will also be made publicly available.

- TimeGAN (Yoon et al., 2019): <https://github.com/jsyoon0823/TimeGAN>
- TimeVAE (Desai et al., 2021): <https://github.com/abudesai/timeVAE>
- TCN-VAE (Krauth et al., 2023): <https://github.com/kruuZHAW/deep-traffic-generation-paper>
- GMM (Barratt et al., 2018): <https://github.com/sisl/terminal-airspace-models>

For TimeGAN, the hidden dimensions of its three GRU layers were set to four times the size of the input features. This setting is consistent with the implementation described in the original TimeGAN paper (Yoon et al., 2019). Moreover, the hidden dimensions of TimeVAE and TCN-VAE were configured to match the hidden dimension used in ATRADA. For both SMOTE-I and SMOTE-E (DeVries & Taylor, 2017), we set the number of nearest neighbors to 10, with the interpolation and extrapolation degrees set at 0.5. Given that SMOTE-I and SMOTE-E were tailored to generate ten times more trajectories than the original data, we only employed the tenth generated sample for each trajectory data point. We used the same number of Gaussian components for the implementation of the GMM as in ATRADA. Furthermore, to tackle the issue of noisy covariance matrices caused by high dimensionality, we utilized the singular value decomposition technique described in the original paper (Barratt et al., 2018).

4.4. Quantitative Evaluation

We performed discriminative and predictive tasks to quantitatively evaluate the quality of the generated aircraft trajectory data. For the discriminative task, we first trained a Transformer-based classifier to distinguish between actual and generated trajectories, labeling the former as *real* and the latter as *fake*. For the classification, we append a classification (CLS) token to the input sequence, an approach borrowed from Bidirectional Encoder Representations from Transformers (BERT) and Vision Transformer (ViT) (Devlin et al., 2019; Dosovitskiy et al., 2021). This CLS token is employed for classifying a given trajectory as either *real* or *fake*. We then computed the discriminative score $|\frac{1}{2} - \text{accuracy}|$ (DS-Classifier). A score closer to zero indicates that the classifier is unable to distinguish between actual and generated trajectories and performs no better than random guessing.

Additionally, we conducted an ATCo Turing test. In the ATCo Turing test, we engaged four professional ATCo who specialize in the airspace of ICN. They were asked to distinguish between real and generated trajectories. Each controller was shown ten trajectory snapshots. Each snapshot displayed both the horizontal view and the vertical profile of the trajectory. Half of these snapshots portrayed real trajectories, while the remaining five displayed generated trajectories. The discriminative score for the ATCo Turing test (DS-ATCo) was computed similarly to the classifier's discriminative score.

Next, we trained a Transformer-based predictor on the generated aircraft trajectory dataset and evaluated its performance on an actual aircraft trajectory dataset, known as the Train

on Synthetic, Test on Real (TSTR) approach. The predictor was designed to predict a future trajectory sequence over a time horizon of 120 seconds given a past trajectory sequence over a time horizon of 120 seconds. For training the predictor, we created pairs of past and future trajectory sequences, each spanning 20 points (120 seconds), by sliding a window with a size of one time step from the generated trajectories. We used the Mean Absolute Error (MAE) to assess the prediction accuracy (PS). Trajectory prediction is one of the major downstream applications of trajectory dataset augmentation, so it is important to validate the usefulness of the generated trajectories based on prediction accuracy.

4.5. Qualitative Evaluation

We applied t-SNE (Van der Maaten & Hinton, 2008) to the datasets of actual and generated aircraft trajectories to visualize how well they match each other. For a deeper analysis, we also applied it to the first and second derivatives of aircraft trajectories (i.e., velocity and acceleration), which allowed us to assess whether the generated trajectories adequately capture the dynamic behavior of aircraft over time. Additionally, we visualized the top view (latitude and longitude) of the generated trajectories, which allowed us to evaluate how well the generated trajectories satisfy various operational constraints, including the designated entry points into the airspace and the FAF that aircraft must pass through to prepare for landing.

5. Results

5.1. Quantitative Evaluation

Table 2 presents the experimental results of the quantitative evaluation. The relative improvements (RIs) were calculated as $|s_2 - s_1| / s_2$ to compare the best score s_1 to the second-best score s_2 . ATRADA performed better than the other baselines and achieved higher RIs of 43.4%, 25.0%, and 36.0% across all three evaluation metrics. This indicates that ATRADA generates trajectories that are more indistinguishable from actual trajectories and more effectively retains their predictive characteristics.

TimeVAE and GMM also performed well. Specifically, the trajectories generated by TimeVAE achieve the second-best score for DS-Classifier metric and the third-best score for DS-ATCo metric. However, they tended to be less effective for predictive tasks compared to ATRADA and GMM. On the other hand, GMM generates trajectories that better preserve the predictive characteristics of the actual trajectories (i.e., lower PS) than TimeVAE, but its discriminative scores are not as strong as those of ATRADA and TimeVAE. SMOTE-I generates trajectories by interpolating two latent vectors and produced trajectories that are similar to actual trajectories, as indicated by strong scores for the DS-

Table 2. Experimental results for three quantitative evaluations. Bold and underlined values indicate the best and second-best performance, respectively.

Model	DS-Classifier	DS-ATCo	PS (Lower the Better)
ATRADA (Ours)	0.013	0.075	0.016
TimeGAN	0.414	0.350	0.084
TimeVAE	<u>0.023</u>	0.125	0.028
SMOTE-I	<u>0.027</u>	<u>0.100</u>	0.056
SMOTE-E	0.176	0.375	0.031
GMM	0.057	0.300	<u>0.025</u>
TCN-VAE	0.036	0.125	0.037
Original	-	-	0.009
RI	43.4%	25.0%	36.0%

Classifier and DS-ATCo metrics. However, these generated trajectories were less useful for predictive tasks. Conversely, the opposite trend occurred with SMOTE-E, which extrapolates two latent vectors to generate synthetic trajectories.

5.2. Qualitative Evaluation

Figure 5 presents the t-SNE visualizations for the position (1st row), velocity (2nd row), acceleration (3rd row) for the generated trajectories from ATRADA, TimeVAE, and GMM, which produced good performance in the quantitative evaluation. The t-SNE visualizations for other baselines can be found in the Appendix A. The trajectories generated by ATRADA exhibit strong overlap with the actual trajectories across all three dimensions. In contrast, a significant portion of the trajectories from TimeVAE and GMM fall out of the distribution for acceleration, which indicates that they do not adequately capture the dynamic behavior of aircraft. Notably, TimeVAE also generates some out-of-distribution samples for position and velocity, which correspond to synthetic trajectories with arbitrary entry points into the airspace, as shown in Figure 6(c).

Figure 6 presents top views of actual and generated trajectories, with entry points and the airport marked by black triangles and squares, respectively. The FAFs for different runway directions are also shown by red “+” symbols. ATRADA and TimeVAE generate smooth aircraft trajectories in the top view, while the trajectories generated by GMM exhibit highly irregular zig-zag patterns that are unrealistic for aircraft movements, as highlighted by the red boxes in Figure 6(d). Furthermore, some of the trajectories generated by TimeVAE spread across the airspace and fail to pass through the designated entry points or the FAF, whereas the trajectories from ATRADA consistently and precisely pass through these points.

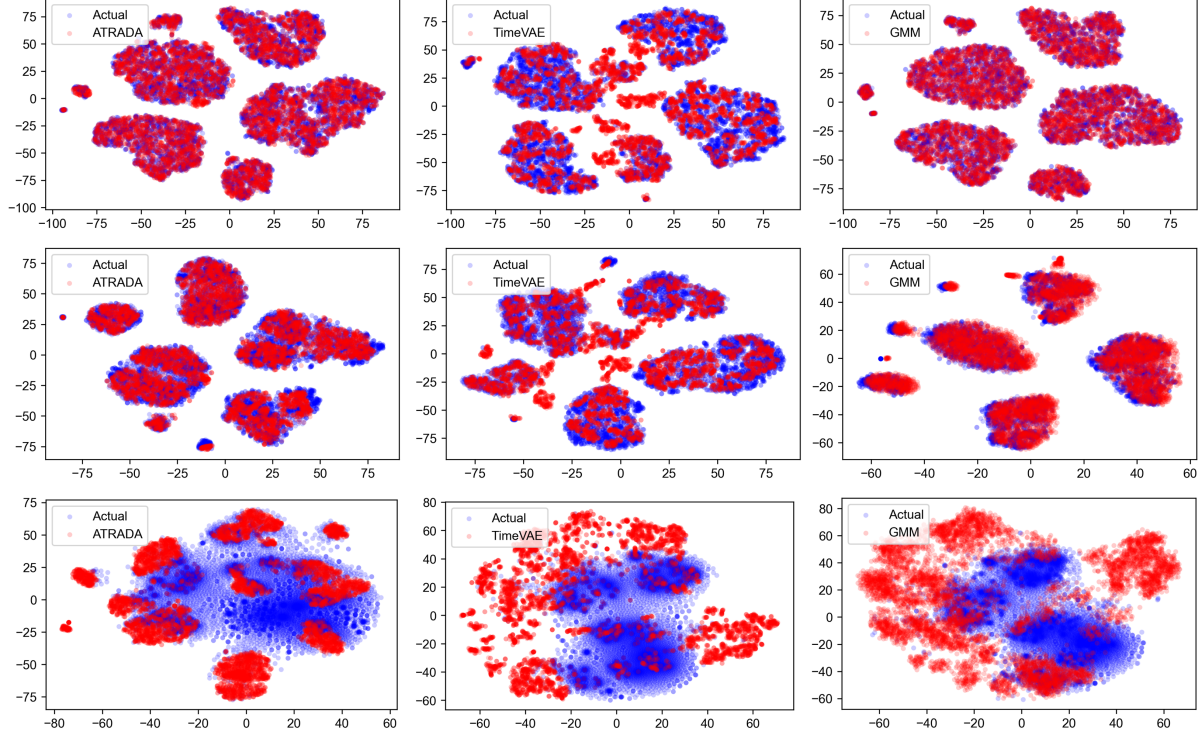


Figure 5. t-SNE visualizations for ATRADA (left), TimeVAE (center), and GMM (right). The t-SNEs for the generated trajectories' position are in the 1st row, velocity (first derivative) in the 2nd row, and acceleration (second derivative) in the 3rd row. Blue indicates the actual trajectories, and red indicates the generated trajectories.

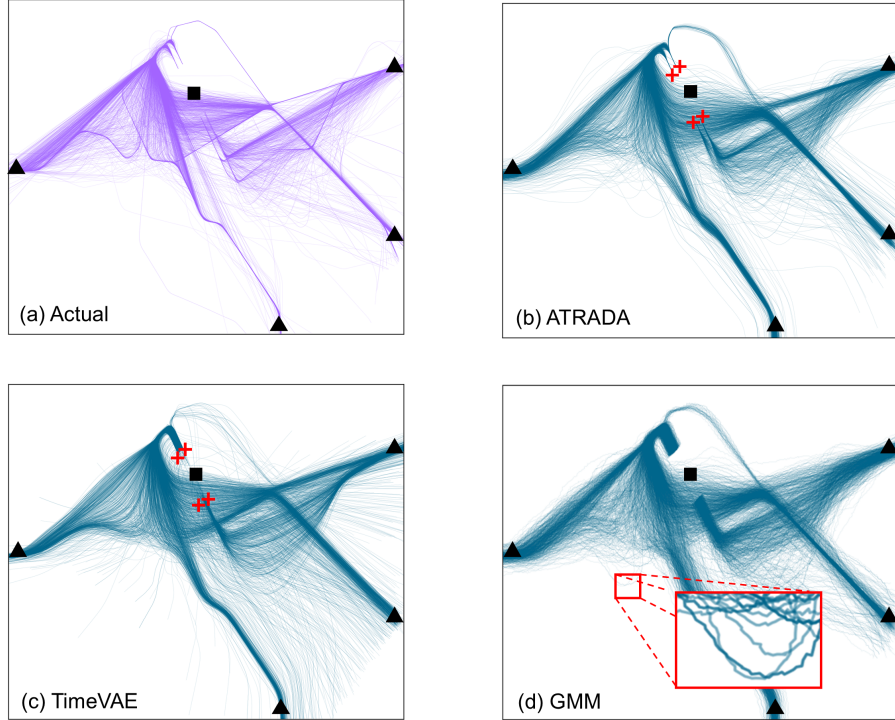


Figure 6. Top view of generated trajectories by ATRADA, TimeVAE, and GMM.

6. Discussion

TimeGAN did not perform well in the task of aircraft trajectory generation despite being considered a state-of-the-art method for time-series data generation. We conjecture that this is due to its implicit likelihood training. Specifically, the generator of TimeGAN is designed to deceive the discriminator rather than accurately learn the probability distribution of the dataset. As a result, the trajectories generated by TimeGAN may fail to satisfy critical spatial constraints, such as designated entry points or STARs in the airspace.

In contrast, models with explicit likelihood training (ATRADA, TimeVAE, TCN-VAE, and GMM) performed better in generating trajectories that align with the spatial distribution of actual trajectories. However, TimeVAE and TCN-VAE still showed limited capability in accurately capturing the distribution of actual trajectories because they learn the dataset’s distribution indirectly through the reconstruction and regularization objectives. Conversely, ATRADA directly estimates the parameters of Gaussian distributions from the actual dataset, which potentially leads to more consistent and reliable trajectory generation.

The idea of using the context vectors in the latent space, rather than the original variables, has proven to offer statistical advantages in many prior works (Bengio et al., 2012; DeVries & Taylor, 2017). The results of this work are also consistent with these findings. Working with GMM in the latent space, rather than in the original input space, allows us to generate synthetic trajectories that are not only more similar to real trajectories but also more beneficial for the downstream tasks, such as trajectory prediction.

7. Conclusion

In this work, we have proposed a novel framework for aircraft trajectory dataset augmentation that leverages the representational capabilities of the Transformer as a sequence autoencoder and the probabilistic nature of the GMM as a generator. The effectiveness of ATRADA was validated using actual air traffic surveillance data. The results demonstrate that it generates more realistic aircraft trajectories that respect the operational constraints of real-world airspace. Given the highly constrained nature of air traffic operations due to safety concerns, the ability of ATRADA to generate trajectories that adhere to both aerodynamic and operational constraints is particularly advantageous. In summary, ATRADA not only exhibits better performance in generating realistic aircraft trajectories, but it could also be beneficial for various downstream tasks such as trajectory prediction and air traffic simulation.

Acknowledgements

This work is supported by the Korea Agency for Infrastructure Technology Advancement (KAIA) grant funded by the Ministry of Land, Infrastructure and Transport (Grant RS-2022-00156364).

References

Barratt, S. T., Kochenderfer, M. J., and Boyd, S. P. Learning probabilistic trajectory models of aircraft in terminal airspace from position data. *IEEE Transactions on Intelligent Transportation Systems*, 20(9):3536–3545, 2018.

Bengio, Y., Mesnil, G., Dauphin, Y., and Rifai, S. Better mixing via deep representations, 2012. URL <https://arxiv.org/abs/1207.4404>.

Chawla, N. V., Bowyer, K. W., Hall, L. O., and Kegelmeyer, W. P. Smote: Synthetic minority over-sampling technique. *Journal of Artificial Intelligence Research*, 16:321–357, 2002.

Desai, A., Freeman, C., Wang, Z., and Beaver, I. Timevae: A variational auto-encoder for multivariate time series generation, 2021. URL <https://arxiv.org/abs/2111.08095>.

Devlin, J., Chang, M.-W., Lee, K., and Toutanova, K. Bert: Pre-training of deep bidirectional transformers for language understanding, 2019. URL <https://arxiv.org/abs/1810.04805>.

DeVries, T. and Taylor, G. W. Dataset augmentation in feature space, 2017. URL <https://arxiv.org/abs/1702.05538>.

Dosovitskiy, A., Beyer, L., Kolesnikov, A., Weissenborn, D., Zhai, X., Unterthiner, T., Dehghani, M., Minderer, M., Heigold, G., Gelly, S., Uszkoreit, J., and Houlsby, N. An image is worth 16x16 words: Transformers for image recognition at scale, 2021. URL <https://arxiv.org/abs/2010.11929>.

Esteban, C., Hyland, S. L., and Rätsch, G. Real-valued (medical) time series generation with recurrent conditional gans, 2017. URL <https://arxiv.org/abs/1706.02633>.

Fritsch, F. N. and Carlson, R. E. Monotone piecewise cubic interpolation. *SIAM Journal on Numerical Analysis*, 17(2):238–246, 1980.

Goodfellow, I. J., Pouget-Abadie, J., Mirza, M., Xu, B., Warde-Farley, D., Ozair, S., Courville, A., and Bengio, Y. Generative adversarial networks, 2014. URL <https://arxiv.org/abs/1406.2661>.

Guo, D., Wu, E. Q., Wu, Y., Zhang, J., Law, R., and Lin, Y. Flightbert: Binary encoding representation for flight trajectory prediction. *IEEE Transactions on Intelligent Transportation Systems*, 24(2):1828–1842, 2022.

Guo, D., Zhang, Z., Yan, Z., Zhang, J., and Lin, Y. Flightbert++: A non-autoregressive multi-horizon flight trajectory prediction framework. In *Proceedings of the AAAI Conference on Artificial Intelligence*, volume 38, pp. 127–134, 2024.

Hong, S. and Lee, K. Trajectory prediction for vectored area navigation arrivals. *Journal of Aerospace Information Systems*, 12(7):490–502, 2015.

Jung, S. and Kochenderfer, M. J. Inferring traffic models in terminal airspace from flight tracks and procedures, 2023. URL <https://arxiv.org/abs/2303.09981>.

Kingma, D. P. and Ba, J. Adam: A method for stochastic optimization, 2017. URL <https://arxiv.org/abs/1412.6980>.

Krauth, T., Lafage, A., Morio, J., Olive, X., and Waltert, M. Deep generative modelling of aircraft trajectories in terminal maneuvering areas. *Machine Learning with Applications*, 11:100446, 2023.

Liu, W. and Hwang, I. Probabilistic trajectory prediction and conflict detection for air traffic control. *Journal of Guidance, Control, and Dynamics*, 34(6):1779–1789, 2011.

Ma, L. and Tian, S. A hybrid cnn-lstm model for aircraft 4d trajectory prediction. *IEEE access*, 8:134668–134680, 2020.

Mogren, O. C-rnn-gan: Continuous recurrent neural networks with adversarial training, 2016. URL <https://arxiv.org/abs/1611.09904>.

Schwarz, G. Estimating the dimension of a model. *The annals of statistics*, pp. 461–464, 1978.

Shi, Z., Xu, M., and Pan, Q. 4-d flight trajectory prediction with constrained lstm network. *IEEE Transactions on Intelligent Transportation Systems*, 22(11):7242–7255, 2020.

Srinivasan, P. and Knottenbelt, W. J. Time-series transformer generative adversarial networks, 2022. URL <https://arxiv.org/abs/2205.11164>.

Sutskever, I., Vinyals, O., and Le, Q. V. Sequence to sequence learning with neural networks. *Advances in neural information processing systems*, 27, 2014.

Tong, Q., Hu, J., Chen, Y., Guo, D., and Liu, X. Long-term trajectory prediction model based on transformer. *IEEE Access*, 2023.

Van der Maaten, L. and Hinton, G. Visualizing data using t-sne. *Journal of machine learning research*, 9(11), 2008.

Vaswani, A., Shazeer, N., Parmar, N., Uszkoreit, J., Jones, L., Gomez, A. N., Kaiser, Ł., and Polosukhin, I. Attention is all you need. *Advances in Neural Information Processing Systems*, 30, 2017.

Yoon, J., Jarrett, D., and Van der Schaar, M. Time-series generative adversarial networks. *Advances in Neural Information Processing Systems*, 32, 2019.

Yoon, S. and Lee, K. Improving aircraft trajectory prediction accuracy with over-sampling technique. In *2023 IEEE/AIAA 42nd Digital Avionics Systems Conference (DASC)*, pp. 1–6. IEEE, 2023.

Yu, B., Lu, P., Wang, R., Hu, W., Tan, X., Ye, W., Zhang, S., Qin, T., and Liu, T.-Y. Museformer: Transformer with fine-and coarse-grained attention for music generation. *Advances in Neural Information Processing Systems*, 35: 1376–1388, 2022.

A. Additional Visualizations

The generated trajectories from all baselines are additionally visualized using t-SNE and 2D plots, as depicted in Figure 7 and Figure 8.

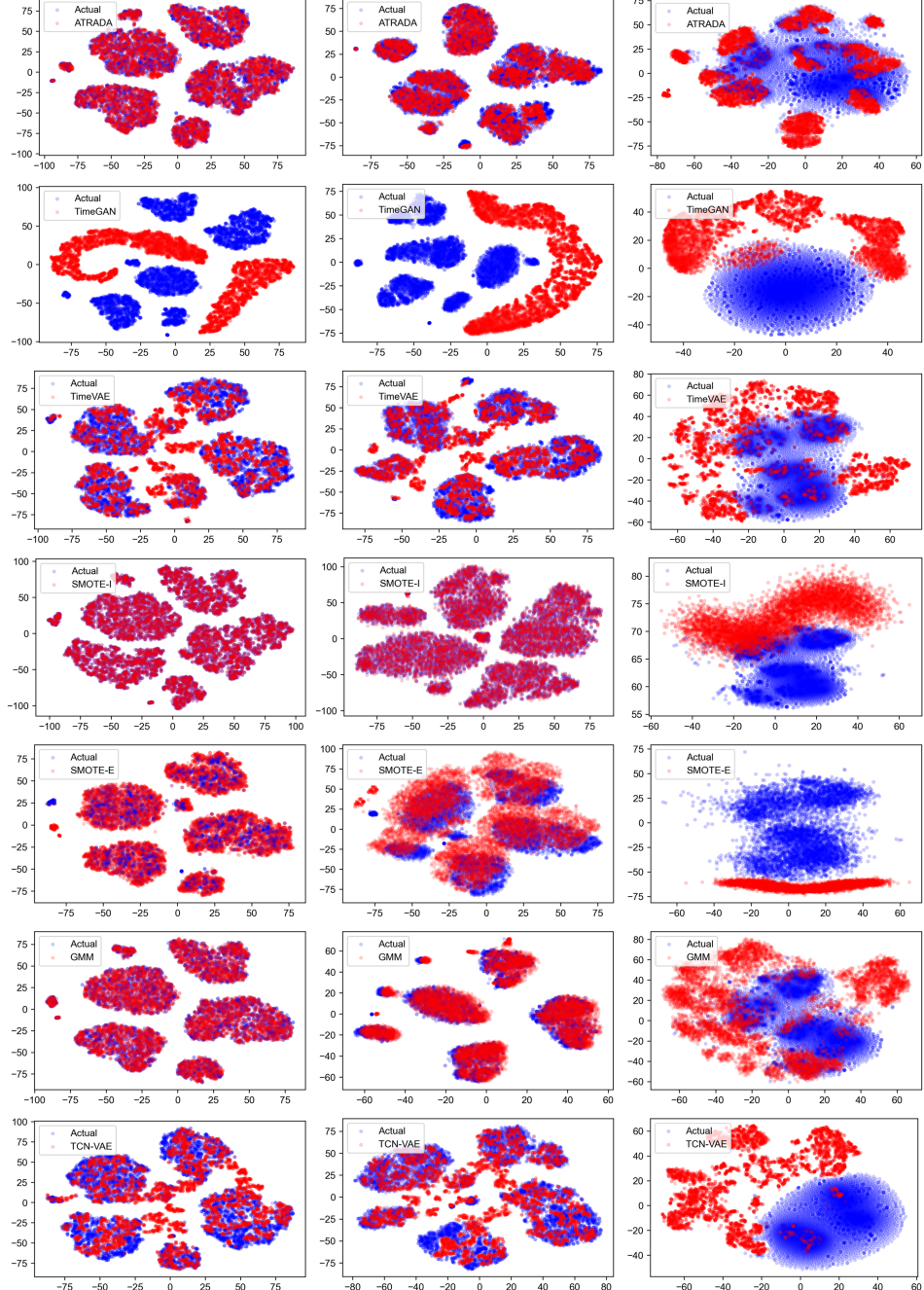


Figure 7. The t-SNE visualizations for ATRADA and all baselines. Each column denotes the generated trajectories' position (1st column), velocity (2nd column), acceleration (3rd column), respectively. Each row depicts the t-SNE visualizations for each method in the following order: (1) ATRADA, (2) TimeGAN, (3) TimeVAE, (4) SMOTE-I, (5) SMOTE-E, (6) GMM, and (7) TCN-VAE. Blue indicates the actual trajectories, while red indicates the generated trajectories.

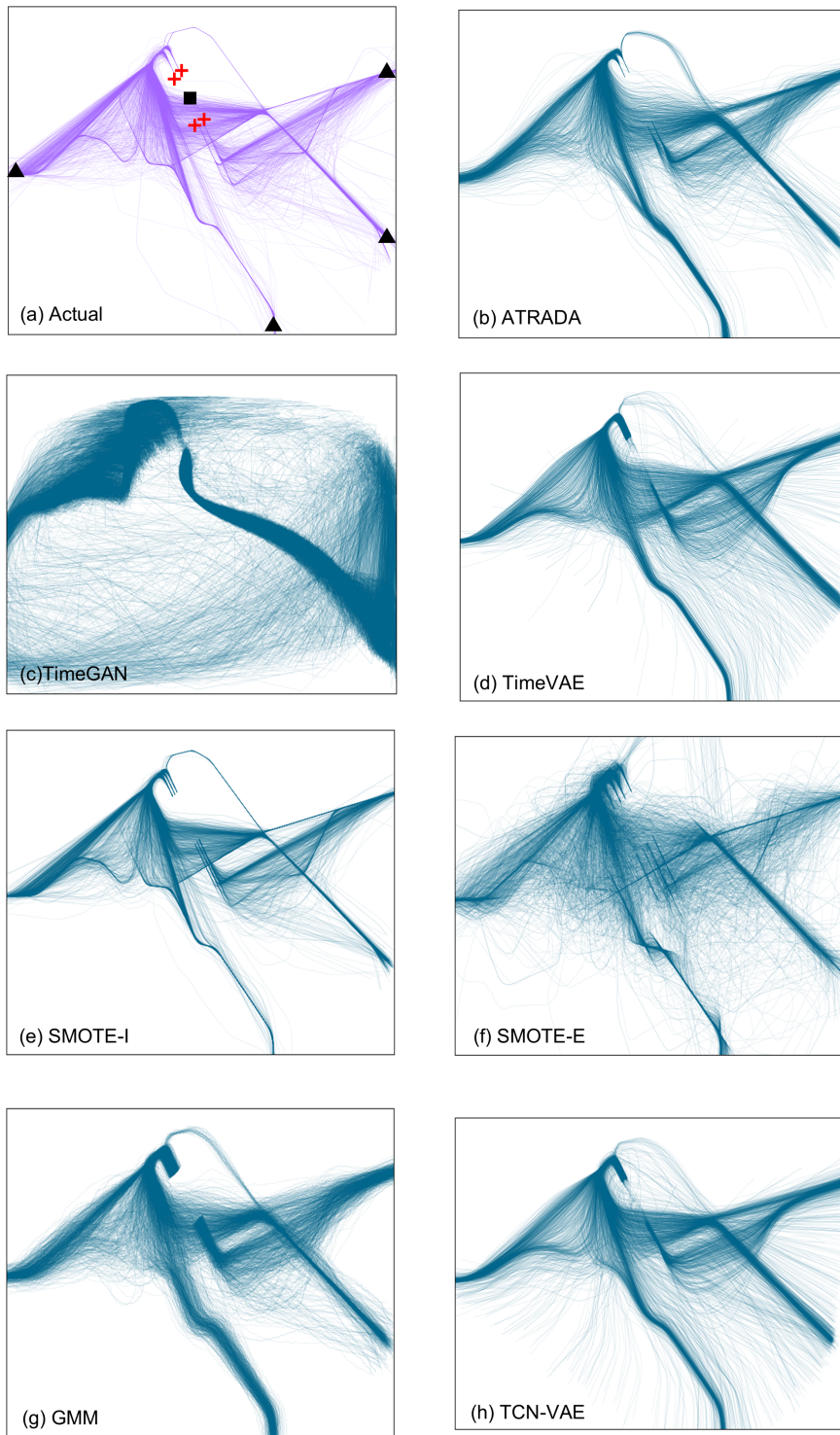


Figure 8. Top view of generated trajectories by ATRADA and all other baselines. The entry points into the airspace and the airport marked by black triangles and squares, respectively. The FAFs for the runway are shown by red "+" symbols.